An Approximate Analytical Solution of Transport Model in Electrodes for Anode-supported Solid Oxide Fuel Cells

Cheng Bao and Ningsheng Cai
Key Laboratory for Thermal Science and Power Engineering of Ministry of Education, Tsinghua University, Beijing 100084, P.R. China

DOI 10.1002/aic.11297
Published online September 27, 2007 in Wiley InterScience (www.interscience.wiley.com).

On the basis of the one-dimensional, isothermal mechanistic model in the anode of an anode-supported solid oxide fuel cell using binary mixture as fuel, two approximate analytical solutions considering both mass and charge transfer were developed in this article. First, by dividing the anode into the inactive and active zones, the regular perturbation method was used to approximate the distribution of the fuel concentration and overpotential. Then the approximate solution using the singular perturbation method reflects both the boundary-layer effects of current density at the two boundaries of the anode. Both the two approximate solutions agree well with the numeric solution in the case of medium and low electric load. By introducing the concept of the boundary-layer thickness at the anode/electrolyte interface, the two approximate solutions can be combined to get an explicit expression in a wide range of operation. The result in this article is useful to system-level modeling and dynamic analysis. © 2007 American Institute of Chemical Engineers *AIChE J,* 53: 2968–2979, 2007
Keywords: solid oxide fuel cell, anode-supported, approximate solution, perturbation method, boundary-layer effect

Introduction

Fuel cells are a kind of environmentally benign, high-efficiency energy conversion devices. As the representative of high-temperature fuel cells with high-quality exhaust energy and considerable fuel flexibility, solid oxide fuel cells (SOFC) is considered to be the most potential candidate for distributed power system, power station, and automotive applications.[1] To alleviate the stringent requirements for the materials at the high temperature, development of new materials, novel cell structure, and reducing operating temperature are presently the main technical approaches. Anode-supported structure has been the mainstream of intermediate temperature planar SOFCs[2] with high power density, in which the anode is much thicker than the electrolyte layer and the cathode.

There are complex mass and heat transfer and electrochemical/chemical phenomena in a fuel cell. In recent years, many numerical SOFC models have been built for detail mechanistic analysis.[3–13] The state-of-the-art mechanistic models have been developed to the multidimensional, nonisothermal, and transient ones based on commercial solvers.[9–12] Although it provides a good understanding of operating principle, these numeric simulations are not suitable for system-level analysis because of their complexity. On the other hand, some semiempirical models are developed to predict the polarization curve,[14,15] which are limited in particular cells and could not represent the detailed impacts of operating and design parameters of SOFC. In the system-level modeling and analysis of system dynamics and control, it requires simple and accurate model of single cells, especially transport model in the membrane/electrolyte assembly.

Correspondence concerning this article should be addressed to N. Cai at cains@tsinghua.edu.cn.

Approximate analytical solution of the transport model provides a good balance between mechanistic and empirical fuel cell models. There have been some literatures in this area. Gurau et al.[16] presented an analytical solution of a transport model for half a polymer electrolyte membrane fuel cell (PEMFC) with the assumption of constant overpotential in the catalyst layer. Thinking the catalyst layer as an infinitely thin interface, Tsai et al.[17] proposed the two-dimensional analytical expression of oxygen transport in the cathode diffusion layer of PEMFC. Costamagna et al.[18] obtained an analytical solution of overpotential distribution in SOFC electrodes by neglecting the variation of concentration and exchange current density. Other researchers[19,20] also developed approximate analytical expressions for channel flow and heat transfer in a fuel cell.

Whatever the structural type and geometry of SOFC, description of mass/charge transfer and electrochemical reaction in porous electrodes is the core of modeling of single cell. By introducing an isothermal, one-dimensional transport model using binary reactants, the purpose of this article is to present an approximate analytical solution using perturbation method. Because of the characteristics of anode-supported SOFCs, the variation of reactant concentration and overpotential are both considerable in the thick electrode. The solving process and analysis is also helpful to understand the phenomena of reaction and diffusion in anode-supported SOFCs.

Transport Model in Electrodes

As shown in Figure 1, the core of SOFC is a "sandwich" structure of positive electrolyte negative (PEN). The electrolyte layer is made from a ceramic such as yttria-stabilized zirconia (YSZ) and plays a role in conducting oxygen ion and separating fuel and oxidant. The material of the anode is typically a Ni-YSZ cermet, and the cathode is mostly lanthanum-based perovskite. Both the electrodes are formed by a mixture of ionic conductor/electronic conductor materials, and porosities are present in the structure for the gas diffusion, ion/electron transport to make the three phase boundary (TPB). At the site of TPB, the electrochemical reaction occurs, which is oxidation of fuel ($H_2 + O^{2-} \rightarrow H_2O + 2e^-$, $CO + O^{2-} \rightarrow CO_2 + 2e^-$) in the anode and reduction of oxygen ($1/2O_2 + 2e^- \rightarrow O^{2-}$) in the cathode, and the current density exchanges between ionic conducting phase and electronic conducting phase. The model is based on the following assumptions:

1. Only steady state is considered;
2. The temperature and pressure are uniform through out the PEN structure;

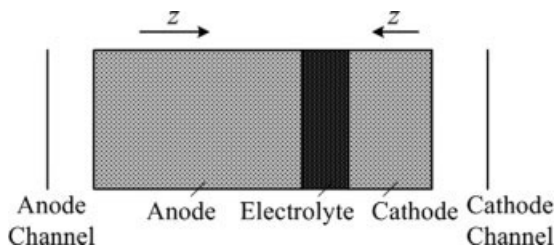

Figure 1. 1D schematic diagram of PEN in anode-supported SOFC.

3. Gases are all ideal gases;
4. Only the z coordinate in the thickness direction of PEN is considered here, and the positive direction is from electrode/channel interface to electrode/electrolyte interface;
5. Each of two conducting phase is considered as continuous and homogeneous, having a conductivity independent of the z coordinate;
6. Considering the small particle size in the electrodes, the interfacial electrical equilibrium is well established[21] (the Wagner number is much higher than 1). So, the interfacial potentials are unnecessary to be distinguished from their phase-averaged counterparts in this macrohomogeneous model.

According to Ohm's law, the charge transfer in electron phase and ion phase are[18]

$$-\sigma_{\text{ion}}^{\text{eff}}\nabla\phi_{\text{ion}} = i_{\text{ion}} \tag{1}$$

$$-\sigma_{\text{el}}^{\text{eff}}\nabla\phi_{\text{el}} = i_{\text{el}} = \psi I - i_{\text{ion}} \tag{2}$$

$$\nabla\cdot i_{\text{ion}} = -\nabla\cdot i_{\text{el}} = \psi j \tag{3}$$

where ϕ, σ, and i are the potential, conductivity, and current density in electronic conducting phase (el) and ionic conducting phase (ion) respectively, I is the operating current density, and ψ represents the exchange of current density between the two phases, i.e., $\psi = 1$ in the anode and $\psi = -1$ in the cathode. The electrochemical reaction rate, j can be described by the general current-overpotential equation[18]

$$j = i_0 S_{\text{TPB}}\left[\frac{C_{\text{react}}}{C_{\text{react,b}}}\exp\left(\frac{\alpha n_e F}{RT}\eta\right) - \frac{C_{\text{prod}}}{C_{\text{prod,b}}}\exp\left(-\frac{\beta n_e F}{RT}\eta\right)\right] \tag{4}$$

where F is the Faraday constant, R the gas constant, T the operating temperature, n_e number of electrons participating in the electrochemical reaction, α and β are the charge transfer coefficients, c_{react}, c_{prod}, $c_{\text{react,b}}$, $c_{\text{prod,b}}$ the reactant and product concentrations at the reaction active sites and bulk concentrations, respectively; S_{TPB} the TPB active area per unit volume of electrode, the exchange current density i_0 is related to the gas concentrations[22]

$$i_0 = i_{0,\text{ref}}\Pi x_i^{\gamma_i} \tag{5}$$

where x_i and γ_i is the molar fraction and reaction order of species i, and the overpotential η is defined as the potential difference between the two phases minus that in equilibrium

$$\eta = \psi\left[\phi_{\text{el}} - \phi_{\text{ion}} - \left(\phi_{\text{el}}^{\text{eq}} - \phi_{\text{ion}}^{\text{eq}}\right)\right] \tag{6}$$

The mass transfer in the porous electrode is described by Stefan-Maxwell equation

$$-\nabla x_i = \sum_{j=1}^{n}\frac{x_j N_i - x_i N_j}{c_t D_{ij}^{\text{eff}}} + \frac{N_i}{c_t D_{i,\text{K}}^{\text{eff}}} \quad (i = 1, 2, \ldots, n) \tag{7}$$

where $c_t = p/R/T$ is the concentration of gas mixture, N_i the diffusion flux of species i, D_{ij}^{eff} the effective binary diffusion coefficient calculated by[23]

$$D_{ij}^{\text{eff}} = D_{ij}\frac{\varepsilon_{\text{P}}}{\tau} = \frac{0.0143}{\sqrt{2000}}\frac{\varepsilon_{\text{P}}}{\tau}\frac{\sqrt{1/M_i + 1/M_j}}{p\left[V_i^{1/3} + V_j^{1/3}\right]^2}\, T^{1.75} \tag{8}$$

where p is the total pressure, M_i the molar mass of species i, ε_{p} the electrode porosity, τ the electrode tortuosity, V_i the special diffusion volume, the effective Knudsen diffusion coefficient of species i, $D_{i,K}^{\text{eff}}$ can be calculated by

$$D_{i,\text{K}}^{\text{eff}} = \frac{2}{3} r_{\text{p}} \frac{\varepsilon_{\text{P}}}{\tau}\sqrt{\frac{8RT}{\pi M_i}} \tag{9}$$

where r_{p} is the mean pore radius of electrode. The mass balance of species is related to the electrochemical reaction rate

$$\nabla \cdot N_i = \upsilon_i \frac{j}{n_e F} + R_i \tag{10}$$

where υ_i is the stoichiometric coefficient of species i in the electrochemical reaction, R_i the reaction rate of species i in other chemical reactions such as internal reforming.

In this article, we just discuss the case using binary mixture (H_2—H_2O, CO—CO_2) as fuel and air as oxidant. It is equimolar counter diffusion ($N_1 = -N_2$) for binary fuel mixture in the anode, and nitrogen is inert ($N_2 = 0$) in the cathode, and only the electrochemical reaction participates ($R_i = 0$). Thus, we can obtain the equations for distribution of reactant's molar fraction (1 = H_2 or CO in the anode, O_2 in the cathode) and overpotential. In the anode, it is

$$\frac{d^2 x_1}{dz^2} = \frac{i_{0,\text{ref}}\, S_{\text{TPB}}}{n_e F c_{\text{t}} D_{1,\text{eff}}} x_1^{\gamma_1}(1 - x_1)^{\gamma_2} \times \left[\frac{x_1}{x_{1,b}}\exp(\alpha f\eta) - \frac{1 - x_1}{1 - x_{1,\text{b}}}\exp(-\beta f\eta)\right] \tag{11}$$

$$\frac{d^2\eta}{dz^2} = \frac{i_{0,\text{ref}}\, S_{\text{TPB}}}{\sigma_{\text{eff}}} x_1^{\gamma_1}(1 - x_1)^{\gamma_2} \times \left[\frac{x_1}{x_{1,\text{b}}}\exp(\alpha f\eta) - \frac{1 - x_1}{1 - x_{1,\text{b}}}\exp(-\beta f\eta)\right] \tag{12}$$

where $f = n_{\text{e}}F/R/T$, the effective diffusion coefficient $D_{1,\text{eff}}$ and the effective conductivity σ_{eff} are

$$\frac{1}{D_{1,\text{eff}}} = \frac{1}{D_{12}^{\text{eff}}} + \frac{1}{D_{1,\text{K}}^{\text{eff}}}, \quad \frac{1}{\sigma_{\text{eff}}} = \frac{1}{\sigma_{\text{el}}^{\text{eff}}} + \frac{1}{\sigma_{\text{ion}}^{\text{eff}}} \tag{13}$$

Neglecting the variation of concentration of oxygen ion, the equations in the cathode are

$$\frac{d^2\left[\ln\left(1 + \frac{D_{12}^{\text{eff}}}{D_{1,\text{K}}^{\text{eff}}} - x_1\right)\right]}{dz^2} = -\frac{i_{0,\text{ref}} S_{\text{TPB}}}{2 n_e F c_1 D_{12}^{\text{eff}}} x_1^{\gamma_1}\left[\frac{x_1}{x_{1,\text{b}}}\exp(\alpha f\eta) - \exp(-\beta f\eta)\right] \tag{14}$$

$$\frac{d^2\eta}{dz^2} = \frac{i_{0,\text{ref}} S_{\text{TPB}}}{\sigma_{\text{eff}}} x_1^{\gamma_1}\left[\frac{x_1}{x_{1,\text{b}}}\exp(\alpha f\eta) - \exp(-\beta f\eta)\right] \tag{15}$$

At the electrode/channel interface ($z = 0$), the concentration of reactant is equal to the bulk concentration, and the ionic current density completely transfers into the electronic current density. At the electrode/electrolyte interface ($z = l$), the flux of reactant is equal to zero, and the electronic current density completely transfers into the ionic current density. So,

$$\begin{aligned} &x_1|_{z=0} = x_{1,\text{b}}, \quad \left.\frac{d\eta}{dz}\right|_{z=0} = -\frac{I}{\sigma_{\text{el}}^{\text{eff}}}, \\ &\left.\frac{dx_1}{dz}\right|_{z=l} = 0, \quad \left.\frac{d\eta}{dz}\right|_{z=l} = \frac{I}{\sigma_{\text{ion}}^{\text{eff}}} \end{aligned} \tag{16}$$

where l is the thickness of the electrode. Define three dimensionless variables as

$$\tilde{z} = z/l, \quad \tilde{x} = x_1/x_{1,\text{b}}, \quad \tilde{\eta} = f\eta \tag{17}$$

Then the system in the anode can be normalized to

$$\frac{d^2\tilde{x}}{d\tilde{z}^2} = \varepsilon_1 x_{1,\text{b}}^{\gamma_1+\gamma_2-1}\tilde{x}^{\gamma_1}\left(\frac{1}{x_{1,\text{b}}} - \tilde{x}\right)^{\gamma_2} \times \left[\tilde{x}\exp(\alpha\tilde{\eta}) - \frac{1 - x_{1,\text{b}}\tilde{x}}{1 - x_{1,\text{b}}}\exp(-\beta\tilde{\eta})\right] \tag{18}$$

$$\varepsilon_2\frac{d^2\tilde{\eta}}{d\tilde{z}^2} = x_{1,\text{b}}^{\gamma_1+\gamma_2}\tilde{x}^{\gamma_1}\left(\frac{1}{x_{1,\text{b}}} - \tilde{x}\right)^{\gamma_2} \times \left[\tilde{x}\exp(\alpha\tilde{\eta}) - \frac{1 - x_{1,\text{b}}\tilde{x}}{1 - x_{1,\text{b}}}\exp(-\beta\tilde{\eta})\right] \tag{19}$$

with the following boundary conditions

$$\tilde{x}|_{\tilde{z}=0} = 1, \quad \left.\frac{d\tilde{\eta}}{d\tilde{z}}\right|_{\tilde{z}=0} = -\frac{Ifl}{\sigma_{\text{el}}^{\text{eff}}}, \quad \left.\frac{d\tilde{x}}{d\tilde{z}}\right|_{\tilde{z}=1} = 0, \quad \left.\frac{d\tilde{\eta}}{d\tilde{z}}\right|_{\tilde{z}=1} = \frac{Ifl}{\sigma_{\text{ion}}^{\text{eff}}} \tag{20}$$

The two constants ε_1 and ε_2 in the above equation are defined as

$$\varepsilon_1 = \frac{i_{0,\text{ref}} S_{\text{TPB}} l^2}{n_e F c_{\text{t}} D_{1,\text{eff}}}, \quad \varepsilon_2 = \frac{\sigma_{\text{eff}}}{i_{0,\text{ref}} S_{\text{TPB}}\, fl^2} \tag{21}$$

which are the two perturbation variables in the next approximate analytical solution. And the transport model in the cathode can be treated similarly.

Approximate Analytical Solution

Because the anode thickness is high in an anode-supported SOFC, the resistance of mass transfer is high and the mass and charge transfer in Eqs. 18–20 should be solved together. The above transport model is strongly nonlinear, and it is hard to obtain the exact analytical solution. Perturbation method is a good approach to approximate analytical solution, which has been widely used in problem of reaction and diffusion and channel flow in fuel cell.[19]

Analysis of perturbation variables

The core of perturbation method is to expand the dominant variables as polynomial expressions of the perturbation

variable.[24] It is important for accurate approximation to find a small or big enough parameter as the perturbation variable. In some cases, the two constants ε_1 or ε_2 can both be probably chosen as the perturbation variable. The values of ε_1 and ε_2 are mainly influenced by the reference volumetric electrochemical reaction rate ($i_{0,\mathrm{ref}}S_{\mathrm{TPB}}$), the electrode thickness, the operating temperature and the ratio of porosity to tortuosity (ε_p/τ). As the product of pressure and diffusivity is constant at a given temperature, ε_1 and ε_2 are independent of the operating pressure. For a SOFC, the typical value of $i_{0,\mathrm{ref}}S_{\mathrm{TPB}}$ is in the order of 10^8–10^{10} A/m^3, ε_p/τ is within the range of 0.02–0.3, and the operating temperature differs from 923–1273 K. However, the electrode thickness in an electrode-supported cell can vary much from 5×10^{-5} to 2×10^{-3} m. As the values of ε_1 and ε_2 are proportional and inversely proportional to the square of the electrode thickness, respectively, they are strongly influenced by the cell size. For example, when using hydrogen as the fuel and the typical values of parameters are $T = 1073.15$ K, $pD_{\mathrm{H_2,H_2O}} = 82$ Pa m^{2}s^{-1}, $\varepsilon_p/\tau = 0.1$, $i_{0,\mathrm{ref}}S_{\mathrm{TPB}} = 1 \times 10^9$A/m^3, $\sigma_{\mathrm{eff}} = 2.27$ S/m, the values of ε_1 and ε_2 should be $\varepsilon_1 = 0.014$, 5.56, and $\varepsilon_2 = 0.042$, 1.05×10^{-4} related to the anode thickness $l = 5 \times 10^{-5}$, 1×10^{-3} m. For an anode-supported SOFC, the constant ε_1 and ε_2 is generally small enough to be chosen as the perturbation variable for the thin cathode and the thick anode, respectively.

On the other hand, there is an important property in the transport model in Eqs. 18 and 19. As the perturbation variable ε_1 is very small, i.e. $\varepsilon_1 \to 0$, the right hand of Eq. 18 approaches to zero, which means the nonlinear equation of fuel concentration approached to a linear one. In this case, the regular perturbation method (RPM) is suitable for the approximate solution. As the perturbation variable ε_2 is very small, i.e. $\varepsilon_2 \to 0$, the left hand of Eq. 19 is close to zero, which means the nonlinear differential equation of overpotential reduced to an algebraic equation. Considering the structural transformation of differential equations, it is a typical problem of boundary layer which is suitable to use the singular perturbation method (SPM) in this case.

Regular perturbation method

From the above analysis of perturbation variable, the regular perturbation method seems not suitable for approximately solving the transport model in the thick anode of an anode-supported SOFC. With the definition of ε_1, we can find that $\Phi = \sqrt{\varepsilon_1}$ is similar to the Thiele modulus which is ratio of the diffusion time constant to the reaction time constant. With the above typical values of parameters ($l = 1 \times 10^{-3}$ m), it follows that $\Phi^2 = 5.56$ (i.e. $\Phi \approx 2.4$) and will be higher when considering the nonlinear items of overpotential in Eq. 18. For a classical problem of diffusion and reaction of gases throughout a porous catalyst pellet in isothermal conditions, generally speaking, if $\Phi^2 > 10$, reaction is much faster than diffusion, and only takes place in a very small thickness of the particle, the remaining being useless. In general, the conductivity of the electronic conductor (Ni) in the anode is far greater than that of the ionic conductor (YSZ), so most of the electrochemical reaction occurs in a zone close to the anode/electrolyte (A/E) interface according to the boundary conditions in Eq. 20. From another point of view, the oxygen ion transferred from the electrolyte layer almost completely participates in the electrochemical reaction in this zone, and the remainder ionic conductor contributes little to the exchange of current densities.

So, we can divide the anode into an active zone and an inactive zone. It is assumed that there is no electrochemical reaction in the inactive zone, and all the electrochemical reaction occurs in the active zone. Thus, the anode in anode-supported SOFCs is similar to the electrode in PEMFCs, in which gas transport in the inactive gas diffusion layer and all the electrochemical reaction occur in the very thin catalyst layer. As a matter of fact, almost all the semiempirical models assume the electrochemical reaction only occurs at the A/E interface.

In the inactive zone, the electrochemical reaction rate is zero ($j = 0$), which means the fuel molar fraction shows linear distribution ($d^2\tilde{x}/d\tilde{z}^2 = 0$). From Eqs. 3 and 10, there is

$$\nabla \cdot (-n_e F N_1 + i_{\mathrm{ion}}) = 0, \quad N_1|_{z=l} = 0, \quad i_{\mathrm{ion}}|_{z=0} = 0, \quad i_{\mathrm{ion}}|_{z=l} = I \tag{22}$$

So, the fuel flux at the anode/channel (A/C) interface is $N_1|_{z=0} = -c_t D_{1,\mathrm{eff}}\, dx_1/dz|_{z=0} = I/n_e F$, and the fuel molar fraction in the inactive zone is expressed as

$$\tilde{x}_{\mathrm{inact}} = 1 - a\tilde{z} = 1 - \frac{Il}{n_e F c_t D_{1,\mathrm{eff}} x_{1,b}}\tilde{z} \tag{23}$$

where $a = Il/(n_e F c_t D_{1,\mathrm{eff}} x_{1,b})$ is the slope rate. And the overpotential in the inactive zone is

$$j = 0 \Rightarrow \tilde{\eta}_{\mathrm{inact}} = \frac{1}{\alpha + \beta}\ln\left[\frac{1 - x_{l,b}\tilde{x}_{\mathrm{inact}}}{(1 - x_{l,b})\tilde{x}_{\mathrm{inact}}}\right] \tag{24}$$

With the coordinate of the inactive/active interface, $\tilde{z}_0$, we can define two new constants

$$\hat{\varepsilon}_1 = \varepsilon_1(1 - \tilde{z}_0)^2, \quad \hat{\varepsilon}_2 = \varepsilon_2/(1 - \tilde{z}_0)^2 \tag{25}$$

Because of the small thickness of the active zone ($1 - \tilde{z}_0$), the RPM is feasible for the transport model in the active zone using $\hat{\varepsilon}_1$ as the perturbation variable. According to the perturbation method, the fuel molar fraction and overpotential are approximated by

$$\tilde{x}(\xi) = \chi_0 + \hat{\varepsilon}_1\chi_1 + o(\hat{\varepsilon}_1), \quad \tilde{\eta}(\xi) - \tilde{\eta}_{\mathrm{inact}}|_{\tilde{z}=\tilde{z}_0} = y_0 + \hat{\varepsilon}_1 y_1 + o(\hat{\varepsilon}_1) \tag{26}$$

By substituting it into Eqs. 18 and 19 and the following boundary conditions in the scale of $\xi = (\tilde{z} - \tilde{z}_0)/(1 - \tilde{z}_0)$

$$\left.\frac{d\tilde{x}}{d\xi}\right|_{\xi=1} = 0., \quad \left.\frac{d\tilde{\eta}}{d\xi}\right|_{\xi=1} = \frac{Ifl(1 - \tilde{z}_0)}{\sigma_{\mathrm{ion}}^{\mathrm{eff}}}, \quad \tilde{x}|_{\xi=0} = 1 - a\tilde{z}_0, \quad \tilde{\eta}|_{\xi=0} = \tilde{\eta}_{\mathrm{inact}}|_{\tilde{z}=\tilde{z}_0} \tag{27}$$

the system can be linearly expanded in series of $\hat{\varepsilon}_1$ according to Taylor expansion and binominal theorem. With the same-order items on both sides of the equation are equivalent, the

system for zero-order fuel molar fraction and overpotential are

$$\begin{cases} \dfrac{d^2\chi_0}{d\xi^2} = 0, & \chi_0|_{\xi=0} = 1 - a\tilde{z}_0, \quad \dfrac{d\chi_0}{d\xi}|_{\xi=1} = 0 \\ \dfrac{d^2y_0}{d\xi^2} = \lambda_0^2 y_0, & y_0|_{\xi=0} = 0, \quad \dfrac{dy_0}{d\xi}\Big|_{\xi=1} = \dfrac{Ifl(1-\tilde{z}_0)}{\sigma_{\text{ion}}^{\text{eff}}} \end{cases} \tag{28}$$

where the item λ_0 is

$$\lambda_0 = \sqrt{\frac{1}{\hat{\varepsilon}_2} x_{\text{l,b}}^{\gamma_1+\gamma_2} \chi_0^{\gamma_1+1} \left(\frac{1}{x_{\text{l,b}}} - \chi_0\right)^{\gamma_2} (\alpha+\beta) \exp\left(\alpha\tilde{\eta}_{\text{act},0}\right)} \tag{29}$$

The analytical solution is obtained as

$$\chi_0(\xi) = 1 - a\tilde{z}_0, \quad y_0(\xi) = C_1[\exp(\lambda_0\xi) - \exp(-\lambda_0\xi)] \tag{30}$$

where the constant C_1 is

$$C_1 = \frac{Ifl(1-\tilde{z}_0)}{\sigma_{\text{ion}}^{\text{eff}}\lambda_0[\exp(\lambda_0) + \exp(-\lambda_0)]} \tag{31}$$

In most cases, only the zero-order overpotential is necessary for accurate calculation. The first-order solution of the fuel molar fraction and overpotential can be obtained similarly in Appendix A. At the inactive/active interface, the derivative of the overpotential should be continuous, that is

$$\frac{dy_0}{d\xi}\Big|_{\xi=0} = 2\lambda_0(\tilde{z}_0).C_1(\tilde{z}_0) = \frac{1}{\alpha+\beta}\frac{a(1-\tilde{z}_0)}{\left[1 - x_{\text{l,b}}(1-a\tilde{z}_0)\right](1-a\tilde{z}_0)} \tag{32}$$

which can used to determine the value of $\tilde{z}_0$ with simple iteration. When the conductivity of the electronic conductor is far greater than that of the ionic conductor, the derivative of the molar fraction distribution can be checked almost continuous at the inactive/active interface.

Up to now, we get an approximate analytical solution using RPM. However, it is hard to get an explicit expression because of the implicit iteration of $\tilde{z}_0$. On the other hand, the overpotential distribution in the inactive zone does not satisfy the boundary condition at the A/C interface. In fact, we did not use the assumption of zero electrochemical reaction rate ($j = 0$) to get the linear overpotential in the inactive zone. Considering the second-order derivative of the overpotential ($\nabla^2\tilde{\eta} > 0$), and its first-order derivative at the two boundaries ($d\tilde{\eta}/d\tilde{z}|_{\tilde{z}=0} < 0, d\tilde{\eta}/d\tilde{z}|_{\tilde{z}=1} > 0$), the overpotential distribution in the anode shows a concave tendency. In addition to the intensive reaction close to the A/E interface, the mismatch of the overpotential at the A/C interface also indicates another boundary-layer effect, which can not be reflected by RPM.

Singular perturbation method

The boundary layer effect at the A/E interface can also be found in the equation of overpotential. Assuming the fuel concentration is uniform and linearly expanding the exponential items in Eq. 19, we can find that $\Gamma = \sqrt{\frac{1}{\varepsilon_2} x_{1,\text{b}}{}^{\gamma_1}\left(1 - x_{1,\text{b}}\right)^{\gamma_2}(\alpha+\beta)}$ is similar to the Thiele modulus in mass transfer. With the above typical values of parameters ($l = 1 \times 10^{-3}$ m, $x_{1,\text{b}} = 0.85$, $\gamma_1 = 0.734$, $\gamma_2 = 0.266$, $\alpha = 1$, $\beta = 0.5$), it follows that $\Gamma \approx 87.5$, which means only a small part of the electrode is utilized. As mentioned earlier, there is another boundary layer effect at the A/C interface. Unlike the constant ε_2 which is dependent on the electrochemical reaction intensity ($i_{0,\text{ref}}S_{\text{TPB}}$) and the electrode thickness, the value of $\varepsilon^2 = \sigma_{\text{eff}}/(n_e F f c_t D_{1,\text{eff}})$ is only related to the operating temperature and the ratio of porosity to tortuosity. With the typical value of $T = 1073.15$ K, $pD_{\text{H}_2,\text{H}_2\text{O}} = 82$ Pa m^2 s^{-1}, $\varepsilon_p/\tau = 0.1$, $\sigma_{\text{eff}} = 2.27$ S/m, the value of $\varepsilon = 0.024$ is also small enough to be chosen as a general perturbation variable here.

In the regular scale of $\tilde{z}$, the outer-boundary solutions at the A/E interface and the A/C interface can be approximated is series of ε

$$\tilde{\eta}_{\text{A/E}}^{o}(\tilde{z}) = \tilde{\eta}_{\text{A/C}}^{o}(\tilde{z}) = Y_0(\tilde{z}) + \varepsilon Y_1(\tilde{z}) + o(\varepsilon) \tag{33}$$

From Eqs. 18–20, there is the following relationship between $\tilde{x}$ and $\tilde{\eta}$

$$\tilde{x}(\tilde{z}) = 1 - b\tilde{z} + \frac{\varepsilon^2}{x_{\text{l,b}}}[\tilde{\eta}(\tilde{z}) - \tilde{\eta}(0)] \quad \left(b = a\sigma_{\text{eff}}/\sigma_{\text{ion}}^{\text{eff}}\right) \tag{34}$$

which can be used to eliminate $\tilde{x}$. With the same-order items on both sides of Eq. B2 are equivalent, the dimensionless overpotential can be obtained as

$$Y_0(\tilde{z}) = \frac{1}{\alpha+\beta}\ln\left[\frac{1 - x_{\text{l,b}}(1-b\tilde{z})}{(1-x_{\text{l,b}})(1-b\tilde{z})}\right], \quad Y_1(\tilde{z}) = 0 \tag{35}$$

Obviously, it does not satisfy the boundary conditions at the A/E and A/C interface. Firstly, we define a new dimensionless coordinate, $\zeta_1 = (1-\tilde{z})/\varepsilon$, to enlarge the boundary layer at the A/E interface.[24] Then, the inner-boundary overpotential at the A/E interface is approximated as

$$\tilde{\eta}_{\text{A/E}}^{\text{i}}(\zeta_1) = \theta_0(\zeta_1) + \varepsilon\theta_1(\zeta_1) + o(\varepsilon) \tag{36}$$

By expanding the outer-boundary solution at the A/E interface in the scale of ζ_1

$$\left(\tilde{\eta}_{\text{A/E}}^{0}\right)^{i}(\zeta_1) = \varphi_0 - \varepsilon\frac{b\zeta_1}{(\alpha+\beta)(1-b)\left[1 - x_{\text{l,b}}(1-b)\right]} \tag{37}$$

where

$$\varphi_0 = \frac{1}{\alpha+\beta}\ln\left[\frac{1 - x_{\text{l,b}}(1-b)}{(1-x_{\text{l,b}})(1-b)}\right] \tag{38}$$

The zero-order item of the inner-boundary solution should be a constant, i.e. $\theta_0(\zeta_1) = \varphi_0$, which is compatible with the system in Eq. B5. From the system of Eq. B6, the first-order overpotential is

$$\theta_1(\zeta_1) = C_5\exp(\lambda_1\zeta_1) + C_6\exp(-\lambda_1\zeta_1) - \frac{b\zeta_1}{(\alpha+\beta)(1-b)\left[1 - x_{\text{l,b}}(1-b)\right]} \tag{39}$$

where $C_5 = 0$ because of the bounded limitation of θ_1 as $\lim_{\varepsilon x \to 0, \tilde{z} \neq 1} \zeta_1 = (1-\tilde{z})/\varepsilon = \infty$, and

$$C_6 = \frac{1}{\lambda_1}\left\{\frac{Ifl}{\sigma_{\text{ion}}^{\text{eff}}} - \frac{b}{(\alpha+\beta)(1-b)\left[1-x_{1,\text{b}}(1-b)\right]}\right\} \tag{40}$$

By expanding Eq. 36 in the scale of $\tilde{z}$, it can be found that the outer expansion of the inner-boundary solution is consistent to the inner expansion of the outer-boundary solution at the A/E interface, i.e. $\left(\tilde{\eta}_{\text{A/E}}^{\text{i}}\right)^o = \left(\tilde{\eta}_{\text{A/E}}^o\right)^i$.

Similarly, the inner-boundary overpotential at the A/C interface can be approximated in an enlarged scale,[24] $\zeta_2 = \tilde{z}/\varepsilon$

$$\tilde{\eta}_{\text{A/C}}^{\text{i}}(\zeta_2) = \vartheta_0(\zeta_2) + \varepsilon\vartheta_1(\zeta_2) + o(\varepsilon) \tag{41}$$

With the expansion of the outer-boundary solution at the A/C interface in the scale of ζ_2

$$\left(\tilde{\eta}_{\text{A/C}}^o\right)^i(\zeta_2) = \varepsilon\frac{b\zeta_2}{(\alpha+\beta)\left(1-x_{1,\text{b}}\right)} \tag{42}$$

there should be $\vartheta_0(\zeta_2) = 0$ which is compatible with the system in Eq. B10. The analytical solution of Eq. B11 is

$$\vartheta_1(\zeta_2) = C_7\exp(\lambda_2\zeta_2) + C_8\exp(-\lambda_2\zeta_2) + \frac{b\zeta_2}{(\alpha+\beta)\left(1-x_{1,\text{b}}\right)} \tag{43}$$

where $C_7 = 0$ because of the bounded limitation of ϑ_1 as $\lim_{\varepsilon \to 0, \tilde{z} \neq 0} \zeta_2 = \tilde{z}/\varepsilon = \infty$, and

$$C_8 = \frac{1}{\lambda_2}\left[\frac{Ifl}{\sigma_{\text{el}}^{\text{eff}}} + \frac{b}{(\alpha+\beta)\left(1-x_{1,\text{b}}\right)}\right] \tag{44}$$

By expanding Eq. 41 in the scale of $\tilde{z}$, the outer expansion of the inner-boundary solution is found also consistent to the inner expansion of the outer-boundary solution at the A/C interface $\left(\text{i.e. } \left(\tilde{\eta}_{\text{A/C}}^{\text{i}}\right)^o = \left(\tilde{\eta}_{\text{A/C}}^o\right)^i\right)$.

So, the explicit expression of the dimensionless overpotential can be obtained by

$$\begin{aligned}\tilde{\eta}(\tilde{z}) &= \tilde{\eta}_{\text{A/C}}^o(\tilde{z}) + \tilde{\eta}_{\text{A/C}}^i(\tilde{z}) + \tilde{\eta}_{\text{A/E}}^i(\tilde{z}) - \left(\tilde{\eta}_{\text{A/C}}^i\right)^o(\tilde{z}) - \left(\tilde{\eta}_{\text{A/E}}^i\right)^o(\tilde{z}) \\ &= Y_0(\tilde{z}) + \varepsilon C_6\exp\left(-\lambda_1\tfrac{1-\tilde{z}}{\varepsilon}\right) + \varepsilon C_8\exp\left(-\lambda_2\tfrac{\tilde{z}}{\varepsilon}\right)\end{aligned} \tag{45}$$

Analysis and Discussion

By using *bvp4c* algorithm of boundary value problems for ordinary differential equations in MATLAB, we can obtain the exact solution of the anode transport model. On a 1.2-GHz PC, it takes almost 0.45 s and 0.65 ms to generate the numerical and approximate analytical solutions. Table 1 lists the parameters in the base case.

As shown in Figures 2a, b, the approximate solutions by the regular and singular perturbation method both agree well with the exact solution in the overall anode. As shown in Figure 2c, there is almost no exchange between the electronic and ionic current density in the most area of the anode, and the ionic current density increases sharply in the zone close to the A/E interface. In the base case, the active zone is ~7% of the anode thickness. The boundary-layer reaction in the thin active zone ensures the accuracy of the two perturbation methods. Figure 2d is the enlarged overpotential distribution in the active zone, there is some discrepancy between the approximate solution and the exact one with the relatively high current density ($I = 2 \times 10^4$ A/m^2). As the current load decreases, the approximate solution will be almost identical to the exact one.

Table 1. Parameters in the Base Case

Descriptions	Symbol	Value
Anode thickness, m	l	1.1×10^{-3}
Ratio of porosity to tortuosity	$\varepsilon_{\text{p}}/\tau$	0.033
Reference volumetric electrochemical reaction rate, A/m^3*	$i_{0,\text{ref}}S_{\text{TPB}}$	4.9414×10^8
H_2—H_2O binary diffusivity, m^2/s[1]	D_{12}	8.1535×10^{-4}
Electronic conductivity, S/m	$\sigma_{\text{el}}^{\text{eff}}$	2×10^6
Ionic conductivity, S/m	$\sigma_{\text{ion}}^{\text{eff}}$	$3.34 \times 10^4 \exp(-10{,}300/T)$
Anode transfer coefficient†	α	1
Cathode transfer coefficient†	β	0.5
H_2 reaction order†	γ_1	0.734
H_2O reaction order†	γ_2	0.266
Operating pressure, Pa	p	1.013×10^5
Operating temperature, K	T	1073.15
Inlet H_2 molar fraction	$x_{1,\text{b}}$	0.85
Operating current density, A/m^2	I	2×10^4

*Interpolated from experiments in Ref. 14.
†From Ref. 8.

In general, the conductivity of the electronic conductor in the anode is far greater than that of the ionic conductor, which makes the boundary-layer effect close to the A/C interface almost invisible. From Eqs. 1–3, the ionic current density is related to the overpotential as

$$i_{\text{ion}} = \frac{\sigma_{\text{el}}^{\text{eff}}\sigma_{\text{ion}}^{\text{eff}}}{\sigma_{\text{el}}^{\text{eff}} + \sigma_{\text{ion}}^{\text{eff}}}\frac{d\eta}{dz} + \frac{\sigma_{\text{ion}}^{\text{eff}}}{\sigma_{\text{el}}^{\text{eff}} + \sigma_{\text{ion}}^{\text{eff}}}I \tag{46}$$

The second item in the above equation reveals the direct-current value of the ionic current density in the inactive zone. As shown in Figure 3b, when the conductivity of the electronic conductor is decreased to be comparable with the conductivity of the ionic conductor, there is a fast increment of the ionic current density to a considerable value close to the A/C interface. In this case, the approximate solution using the singular perturbation method clearly reflects the concave tendency of the overpotential as shown in Figure 3a. Undoubtedly, the decrement of the conductivity of the electronic conductor will lead to higher overall overpotential and lower rated operating current density.

From, the variation of overpotential is obtained by

$$\begin{aligned}\frac{d\tilde{\eta}}{d\tilde{z}}\Big|_{\tilde{z}=\tilde{z}_{\text{b}}} \approx{}& \lambda_1 C_6\exp\left(-\lambda_1\frac{1-\tilde{z}_{\text{b}}}{\varepsilon}\right) \\ &+ \frac{1}{\alpha+\beta}\frac{b(1-\tilde{z}_{\text{b}})}{\left[1-x_{1,\text{b}}(1-b\tilde{z}_{\text{b}})\right](1-b\tilde{z}_{\text{b}})}\end{aligned} \tag{47}$$

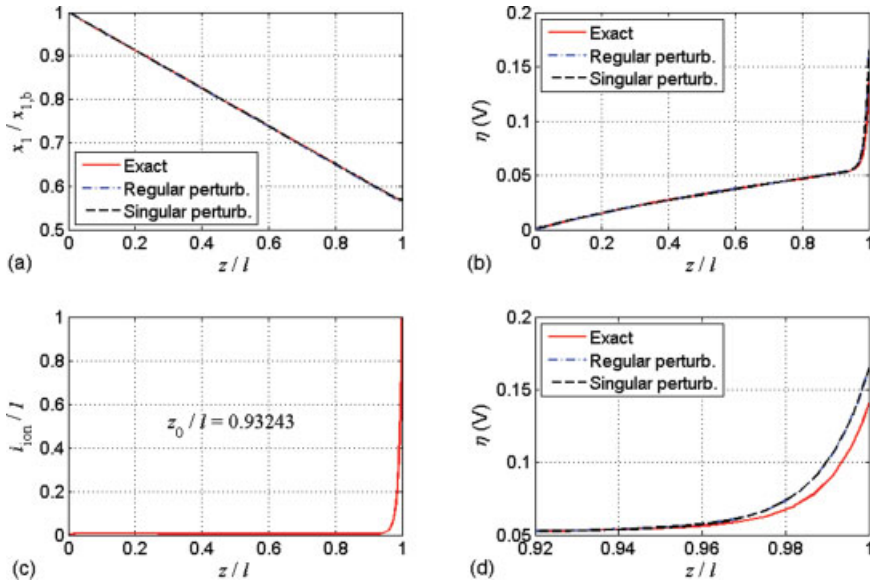

Figure 2. Comparison between the exact (numeric) solution and the approximation solutions by using the regular perturbation method and the singular perturbation method.

(a) Distribution of the dimensionless hydrogen molar fraction. (b) Distribution of the overpotential in the overall anode. (c) Distribution of the dimensionless ionic current density. (d) Distribution of the overpotential in the active zone of the anode. [Color figure can be viewed in the online issue, which is available at www.interscience.wiley.com.]

Similar to the definition of boundary layer of fluids, we can introduce the concept of boundary layer close to the A/E interface. Assuming 99% variation of the ionic current density occurs in the boundary layer, it can be found from Eq. 46 that the derivative of the overpotential at the coordinate of the boundary layer ($\tilde{z} = \tilde{z}_b$) is 1% of that at the A/E interface. The dot–dash line in Figure 3b represents the threshold dimensionless ionic current density. Considering the effect of fuel bulk concentration on the boundary-layer thickness, it can be obtained from Eq. 45

$$\left.\frac{d\tilde{\eta}}{d\tilde{z}}\right|_{\tilde{z}=\tilde{z}_b} = (0.01 - 0.01x_{1,b})\frac{Ifl}{\sigma_{ion}^{eff}} \Rightarrow \tilde{z}_b \approx 1 + \frac{\varepsilon}{\lambda_1}\ln(0.01 - 0.01x_{1,b}) \tag{48}$$

Figure 4 shows the influence of some parameters on the values of $\tilde{z}_0$ and $\tilde{z}_b$, respectively in the case of different operating current density and fuel bulk concentration. The trend of these two values can be analyzed from the effect of the parameter on the electrochemical reaction rate. At a given operating current density, when the reference electrochemical reaction rate increases, or fuel and product reaction order decreases, the reaction rate increases and the majority of electrochemical reaction occurs closer to the A/E interface. Then, the dimensionless ionic current density (i_{ion}/I) will slowly increase more to the threshold value (1%), i.e., the dimensionless thickness of the inactive zone increases. With the higher operating current density, it requires higher thickness of the active zone or the A/E boundary layer. In the

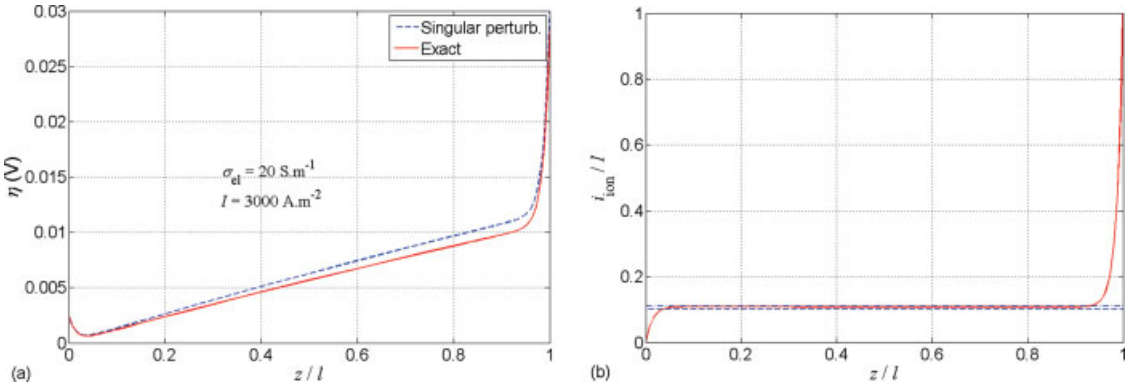

Figure 3. Effect of the conductivity of the electronic conductor on the boundary-layer effect at the channel/anode interface.

(a) Distribution of the overpotential, (b) distribution of the ionic current density. In this case, the conductivity of the electronic conductor is just 20 S/m, and the operating current density is I = 3000 A/m^2, other parameters are the same as those in Table 1. The dash line in (b) represents the second item in Eq. 46, and the dot–dash line is for the threshold of dimensionless ionic current density. [Color figure can be viewed in the online issue, which is available at www.interscience.wiley.com.]

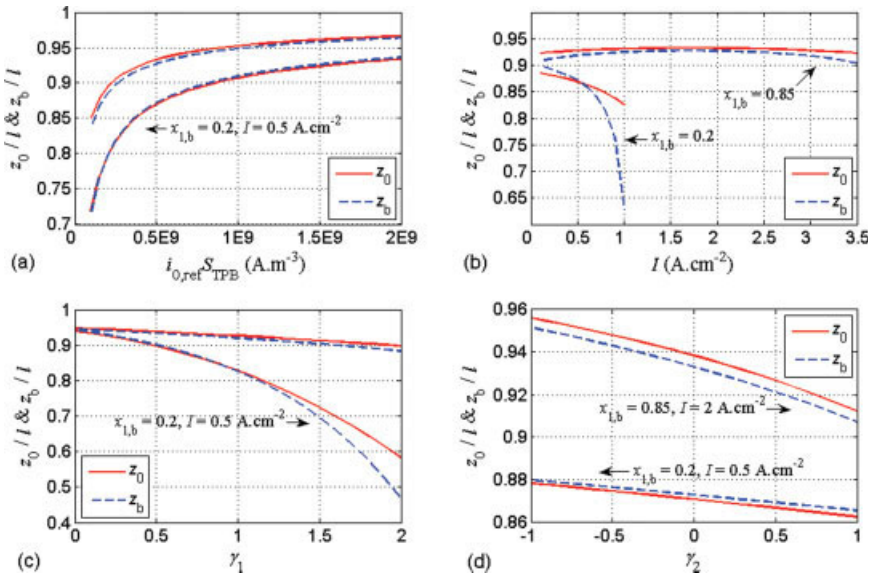

Figure 4. Effects of parameters on the values of $\tilde{z}_0$ and $\tilde{z}_b$ in two cases, $x_{1,b}$ = 0.85, I = 2 A/cm^2 and $x_{1,b}$ = 0.2, I = 0.5 A/cm^2.

(a) Reference electrochemical reaction rate. (b) Operating current density. (c) Fuel reaction order and (d) is for product reaction order. Other parameters are the same as those in Table 1. [Color figure can be viewed in the online issue, which is available at www.interscience.wiley.com.]

case of low fuel concentration, the high resistance of mass transfer makes it more obvious. As shown in Figure 4b, the values of $\tilde{z}_0$ and $\tilde{z}_b$ is almost not influenced by the electric load when the fuel concentration is high, while they get influenced much by the operating current density at low fuel concentration.

It is found that the approximate solution using RPM is more accurate than that using SPM in most cases. As shown in Figure 4, there is good agreement between the values of $\widetilde{z}_0$ and $\widetilde{z}_b$ except the cases of high operating current density and low fuel molar fraction. By replacing $\widetilde{z}_0$ with $\widetilde{z}_b$, we can combine the two approximate analytical solutions of the transport model, which can reflect the boundary layers at two interfaces and avoid the implicit iteration of $\widetilde{z}_0$. Thus, the following explicit expression of overpotential is valid in a wide range

$$\begin{cases} \eta(\tilde{z} \le \tilde{z}_b) = \dfrac{1}{f(\alpha+\beta)} \ln\left[\dfrac{1-x_{1,b}(1-b\tilde{z})}{(1-x_{1,b})(1-b\tilde{z})}\right] + \frac{\varepsilon C_8}{f} \exp\left(-\lambda_2 \frac{\tilde{z}}{\varepsilon}\right) \\ \eta(\tilde{z} > \tilde{z}_b) = \dfrac{2C_1}{f} \sinh\left(\lambda_0 \dfrac{\tilde{z}-\tilde{z}_b}{1-\tilde{z}_b}\right) \end{cases} \tag{49}$$

The overall overpotential, η_t can be obtained by integrating the transport model

$$\begin{aligned} \eta_t &= \phi_{el}(0) - \phi_{ion}(1) - \left(\phi_{el}^{eq} - \phi_{ion}^{eq}\right) \\ &= \frac{\sigma_{ion}^{eff}}{\sigma_{el}^{eff}+\sigma_{ion}^{eff}}\eta(0) + \frac{\sigma_{el}^{eff}}{\sigma_{el}^{eff}+\sigma_{ion}^{eff}}\eta(1) + \frac{Il}{\sigma_{el}^{eff}+\sigma_{ion}^{eff}} \end{aligned} \tag{50}$$

As $\sigma_{el}^{eff} \gg \sigma_{ion}^{eff}$, the overall overpotential can be approximated by $\eta_t \approx \eta(1) = 2C_1\sinh(\lambda)/f$.

We define the effectiveness factor, Θ, as the ratio between the overall electric current effectively supplied by the anode and the overall electric current that would be supplied in the case where the fuel concentration and the overpotential would be uniformly equal to the bulk fuel concentration and the overall overpotential on the overall anode, respectively

$$\begin{aligned} \Theta &= \frac{\int_0^l j(x_1,\eta)dz}{j(x_{1,b},\eta_t)} = \frac{\sigma_{eff}/l}{j(x_{1,b},\eta_t)}\left[\left.\frac{d\eta}{dz}\right|_{z=l} - \left.\frac{d\eta}{dz}\right|_{z=0}\right] \\ &= \frac{I}{i_{0,ref}S_{TPB}lx_{1,b}^{\gamma_1}(1-x_{1,b})^{\gamma_2}[\exp(\alpha f\eta_t) - \exp(-\beta f\eta_t)]} \end{aligned} \tag{51}$$

Figure 5 shows the anode effectiveness factor with variation of some parameters. Here, the catalyst utilization ratio of the anode is almost only 1%, which is consistent with the above concept of A/E boundary layer. Further, when we neglect the variation of fuel concentration (b = 0), there is $\lambda_1/\varepsilon = \sqrt{\frac{1}{\varepsilon_2}x_{1,b}^{\gamma_1}(1-x_{1,b})^{\gamma_2}(\alpha+\beta)}$, which is equal to the Thiele number (Γ) with the linearly expansion of the exponential items. Then, the overall effectiveness factor will be almost inversely proportional to the Thiele number ($\Theta \approx 1/\Gamma$) and the active zone thickness is

$$1 - \tilde{z}_b \approx -\Theta\ln(0.01 - 0.01x_{1,b}) \tag{52}$$

The approximate solution of the transport model in the cathode can also be obtained using the RPM. However, from Eqs. 14 and 15, the two constants similar to the Thiele modulus are

$$\Phi = \sqrt{\frac{i_{0,ref}S_{TPB}l^2}{2n_eFc_tD_{12}^{eff}}}, \quad \Gamma = \sqrt{i_{0,ref}S_{TPB}fl^2x_{1,b}^{\gamma_1}(\alpha+\beta)/\sigma_{eff}} \tag{53}$$

With the typical values as T = 1073.15 K, pD_{O_2,N_2} = 19.3 Pa m^2 s^{-1}, ε_p/τ = 0.1, $i_{0,ref}S_{TPB}$ = 1 × 10^{9}A/m^3, l =

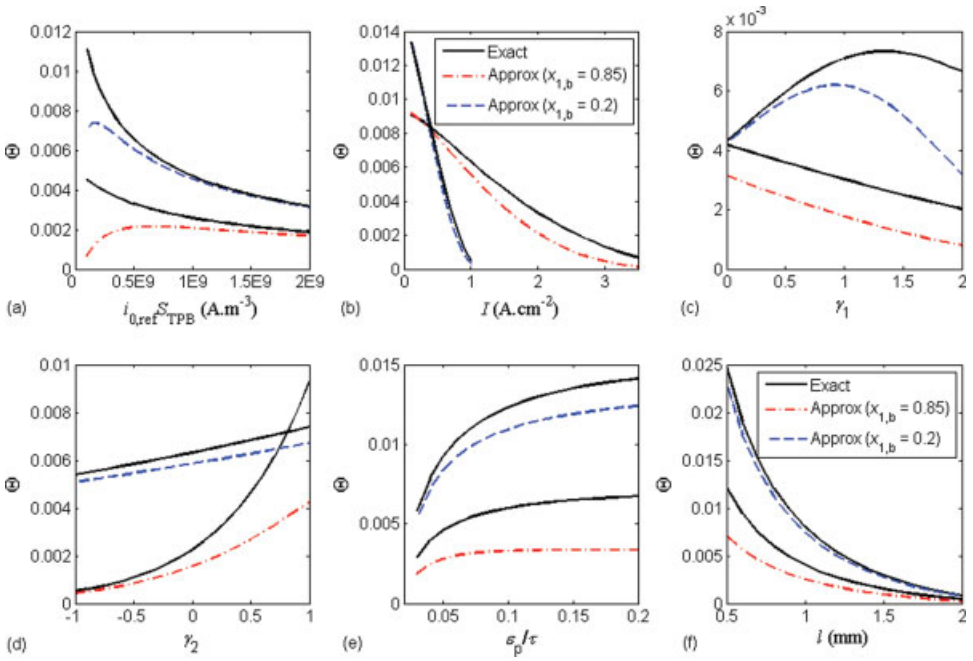

Figure 5. Effects of parameters on the anode effectiveness factor in two cases, $x_{1,b}$ = 0.85, I = 2 A/cm^2 and $x_{1,b}$ = 0.2, I = 0.5 A/cm^2.

(a) Reference electrochemical reaction rate. (b) Operating current density. (c) Fuel reaction order. (d) Product reaction order. (e) Ratio of porosity to tortuosity and (f) anode thickness. Other parameters are the same as those in Table 1. [Color figure can be viewed in the online issue, which is available at www.interscience.wiley.com.]

5×10^{-5} m, it follows that $\Phi \approx 0.17$ (i.e. $\Phi^2 < 0.1$), which means diffusion is much faster than reaction, and consequently the reactant concentration in the electrode can be considered as uniform. For a cathode using air, oxygen is diluted by inert nitrogen and air flow rate is usually big for cooling the cell, so it is reasonable to neglect the variation of oxygen concentration in the thin cathode of an anode-supported SOFC.

If the overall overpotential is not high, we can obtain the analytical solution of overpotential by linearization of the exponent item in Eq. 15, which has been discussed detailed in Ref. 18

$$\eta(\tilde{z}) = \frac{Il}{\Gamma \sinh(\Gamma)} \left\{ \frac{1}{\sigma_{\text{ion}}^{\text{eff}}} \cosh(\Gamma \tilde{z}) + \frac{1}{\sigma_{\text{el}}^{\text{eff}}} \cosh[\Gamma(1-\tilde{z})] \right\} \quad (54)$$

As $x_1 = x_{1,b}$, the implicit analytical solution of Eq. 15 is

$$\frac{d\tilde{\eta}}{d\tilde{z}} = \sqrt{\frac{2\Gamma^2}{\alpha+\beta}} \left[\frac{1}{\alpha} \exp(\alpha\tilde{\eta}) + \frac{1}{\beta} \exp(-\beta\tilde{\eta}) \right] + C \quad (55)$$

When $\sigma_{\text{el}}^{\text{eff}} \gg \sigma_{\text{ion}}^{\text{eff}}$, the overpotential at the cathode/channel interface is far less than that at the cathode/electrolyte interface [i.e., $\eta(0) \approx 0$, $\eta(1) \gg \eta(0)$]. Further, we can obtain the approximate overall overpotential in the cathode when the electric load is high

$$\eta_1 \approx \eta(1) \approx \frac{1}{\alpha f} \ln \left[\frac{\alpha(\alpha+\beta)}{2\Gamma^2} \left(\frac{Ifl}{\sigma_{\text{ion}}^{\text{eff}}} \right)^2 + 1 + \frac{\alpha}{\beta} \right] \quad (56)$$

Conclusion

Both the mass and charge transfer should be considered in the transport model in electrodes of SOFC, especially for the thick electrode with high diffusion resistance. Aiming at the 1D isothermal transport model in the electrodes of an anode-supported SOFC using binary mixture as fuel, two approximate analytical solutions using perturbation methods were developed in this article. Both the two approximate solutions agree well with the numeric solution in the case of medium and low electric load.

On the basis of RPM, the distribution of the fuel concentration and overpotential were approximated by dividing the anode into the inactive zone and active zone. Then the other approximate solution using SPM clearly reflects the two boundary-layer phenomena of current density distribution close to the A/C and A/E interface. Being consistent to the low effective factor of the anode in an anode-supported SOFC, the concept of boundary-layer thickness at A/E interface can be used to get the combined approximate solution in Eq. 49, which avoid the implicit iteration in RPM and get more accurate than that using SPM. And the overall overpotential in the cathode is also approximately obtained in the high electric load.

The results in this article can be used to simplify distribution-parameter modeling of SOFCs and analysis of system dynamics and control.

Notation

a,b = slope rate of dimensionless fuel concentration
c = concentration (mol/m^3)
C = constants

D = diffusivity (m^2/s)
$f = n_e F/R/T$ (V^{-1})
F = Faraday's constant (96487 C/mol)
i_0 = exchange current density (A/m^2)
I = operating current density (A/m^2)
j = electrochemical reaction rate (A/m^3)
l = electrode thickness (m)
M = molecular weight (kg/mol)
n_e = electrons transferred per reacting molecule ($n_e = 2$)
N = flux (mol m^{-2} s^{-1})
p = pressure (Pa)
r_p = mean pore radius of electrode
R = universal gas constant (8.314 J mol^{-1} K^{-1})
S_{TPB} = active area of triple phase boundary (TPB) per unit volume (m^2/m^3)
T = temperature (K)
x = molar fraction
$x_{1,b}$ = fuel or oxygen bulk molar fraction
$\tilde{x}$ = dimensionless molar fraction
z = spatial coordinate along the electrode thickness (m)
$\tilde{z}$ = dimensionless z coordinate
$\tilde{z}_0$ = dimensionless thickness of the inactive zone
$\tilde{z}_b$ = dimensionless coordinate of boundary layer at A/E interface

Greek letters

α = anode transfer coefficient
β = cathode transfer coefficient
ε_p = porosity of electrode
ε_1, ε_2, ε = perturbation variables
η = overpotential (V)
$\tilde{\eta}$ = dimensionless overpotential
γ = reaction order
φ = potential (V)
σ = conductivity (S/m)
τ = tortuosity
ξ = dimensionless coordinate for the active zone
ζ_1, ζ_2 = dimensionless coordinates for enlarged boundary layers
Γ = dimensionless parameter for charge transfer
Φ = dimensionless parameter for mass transfer
ψ = positive direction of current density ($\psi = 1$ in anode, $\psi = -1$ in cathode)
Θ = effectiveness factor of electrode

Subscripts and superscripts

A/C = anode/channel interface
A/E = anode/electrolyte interface
eff = effective
el = electronic conducting phase
eq = equilibrium
K = Knudsen
i = species or inner expansion of boundary-layer solution
ion = ionic conducting phase
t = total or overall
o = outer expansion of boundary-layer solution

Literature Cited

1. Lamp P, Tachtler J, Finkenwirth O, Finkenwirth O, Mukerjee S, Shaffer S. Development of an auxiliary power unit with solid oxide fuel cells for automotive applications. *Fuel Cells*. 2003;3:146–152.
2. Hirschenhofer JF, Stauffer DB, Engleman RR. *Fuel Cell Hand Book*, 7th ed. Morgantown: U.S. Department of Energy, 2004.
3. Debendetti PG, Vayenas CG. Steady-state Analysis of high temperature fuel cells. *Chem Eng Sci*. 1983,38:1817–1829.
4. Achenbach E. Three-dimensional and time dependent simulation of a planar solid oxide fuel cell stack. *J Power Sources*. 1994,49:333–348.
5. Bessette NF II, Wepfer WJ, Winnick J. A mathematical model of a solid oxide fuel cell. *J Electrochem Soc*. 1995,142:3792–3800.
6. Ferguson JR, Fiard JM, Herbin R. Three-dimensional numerical simulation for various geometries of solid oxide fuel cells. *J Power Sources*. 1996,58:109–122.
7. Costamagna P, Honegger K. Modeling of solid oxide heat exchanger integrated stacks and simulation at high fuel utilization. *J Electrochem Soc*. 1998,145:3995–4007.
8. Nagata S, Momma A, Kato T, Kasuga Y. Numerical analysis of output characteristics of tubular SOFC with internal reformer. *J Power Sources*. 2001,101:60–71.
9. Yakabe H, Ogiwara T, Hishinuma M, Yasuda I. 3-D model calculation for planar SOFC. *J Power Sources*. 2001,102:144–154.
10. Aguiar P, Chadwick D, Kershenbaum L. Modeling of an indirect internal reforming solid oxide fuel cell. *Chem Eng Sci*. 2002,57:1665–1677.
11. Ackmann T, DeHarrt LGL, Lehnert W, Stolten D. Modeling of mass and heat transport in planar substrate type SOFCs. *J Electrochem Soc*. 2003,150:A783–A789.
12. Recknagle KP, Williford RE, Chick LA, Rector DR, Khaleel MA. Three-dimensional thermo-fluid electrochemical modeling of planar SOFC stacks. *J Power Sources*. 2003,113:109–114.
13. Li PW, Chyu MK. Electrochemical and transport phenomena in solid oxide fuel cells. *J Heat Transfer*. 2005,127:1344–1362.
14. Kim JW, Virkar AV, Fung KZ, Mehta K, Singhal SC. Polarization effects in intermediate temperature, anode-supported solid oxide fuel cells. *J Electrochem Soc*. 1999,146:69–78.
15. Celik I, Pakalapati SR, Villalpandao MDS. Theoretical calculation of the electrical potential at the electrode-electrolyte interfaces of solid oxide fuel cells. *J Fuel Cell Sci Technol*. 2005,2:238–245.
16. Gurau V, Barbir F, Liu H. An analytical solution of a half-cell model for PEM fuel cells. *J Electrochem Soc*. 2000,147:2468–2477.
17. Tsai CR, Chen F, Ruo AC, Chang MH, Chu HS, Soong CY, Yan WM, Cheng CH. An analytical solution for transport of oxygen in cathode gas diffusion layer of PEMFC. *J Power Sources*. 2006, 160:50–56.
18. Costamagna P, Costa P, Antonucci V. Micro-modelling of solid oxide fuel cell electrodes. *Electrochimica Acta*. 1998,43:375–394.
19. Sung Y. An approximate analytical solution to channel flow in a fuel cell with a draft angle. *J Power Sources*. 2006,159:1051–1060.
20. Coutelieris FA, Douvartzides SL, Tsiakaras PE. Heat transfer phenomena in a solid oxide fuel cell: an analytical approach. *Chem Eng Sci*. 2005,60:4423–4430.
21. Wang CY, Gu WB, Liaw BY. Micro-macroscopic coupled modeling of batteries and fuel cells. Part I. Model development. *J Electrochem Soc*. 1998,145:3407–3417.
22. Zhu H, Kee RJ. A general mathematical model for analyzing the performance of fuel-cell membrane-electrode assemblies. *J Power Sources*. 2003,117:61–74.
23. Todd B, Young JB. Thermodynamic and transport properties of gases for use in solid oxide fuel cell modelling. *J Power Sources*. 2002,110:186–200.
24. Nayfeh AH. *Introduction to Perturbation Techniques*. New York: Wiley, 1981.

Appendix A: First-Order Solution for RPM

According to Taylor expansion and binominal theorem, the two following nonlinear equations are approximated in series of perturbation variable (ε)

$$(g+\varepsilon h)^{\gamma} \approx g^{\gamma} + \varepsilon\gamma g^{\gamma-1} h, \quad \exp[g+\varepsilon h] \approx \exp(g)(1+\varepsilon h) \tag{A1}$$

Similar to the zero-order equations, the system of the first-order fuel molar fraction is

$$\frac{d^2\chi_1}{d\xi^2} = \frac{\hat{\varepsilon}_2\lambda_0^2}{x_{1,b}} y_0, \quad \chi_1|_{\xi=0} = 0, \quad \left.\frac{d\chi_1}{d\xi}\right|_{\xi=1} = 0. \tag{A2}$$

Thus, it can be obtained

$$\chi_1(\xi) = \frac{\hat{\varepsilon}_2 C_1}{x_{1,b}} [\exp(\lambda_0\xi) - \exp(-\lambda_0\xi)] - C_2\xi \tag{A3}$$

where the constant C_2 is

$$C_2 = \hat{\varepsilon}_2 Ifl(1-\tilde{z}_0)/x_{1,b}\sigma_{ion}^{eff} \tag{A4}$$

The system of the first-order overpotential is

$$\frac{d^2y_1}{d\xi^2} = \lambda_0^2 y_1 + \lambda_0^2 k_1 y_0 \chi_1 + \lambda_0^2 k_2 \chi_1, \quad y_1|_{\xi=0} = 0, \quad \frac{dy_1}{d\xi}|_{\xi=1} = 0 \tag{A5}$$

where the item k_1 and k_2 are

$$k_1 = \frac{\frac{\alpha}{\alpha+\beta} + \gamma_1 - (\gamma_1+\gamma_2+1)x_{1,b}\chi_0}{\chi_0(1-x_{1,b}\chi_0)}, \qquad k_2 = \frac{1}{n_e(\alpha+\beta)\chi_0(1-x_{1,b}\chi_0)} \tag{A6}$$

The analytical solution can be obtained by

$$\begin{aligned} y_1(\xi) = {} & C_3\exp(\lambda_0\xi) + C_4\exp(-\lambda_0\xi) \\ & + \frac{2k_1\hat{\varepsilon}_2 C_1^2}{x_{1,b}}\left[\frac{1}{3}\cos h(2\lambda_0\xi) + 1\right] \\ & - \frac{k_1 C_1 C_2}{4\lambda_0}\left[\left(2\lambda_0^2\xi^2+1\right)\cos h(\lambda_0\xi) - 2\lambda_0\xi\sin h(\lambda_0\xi)\right] \\ & + \frac{k_2\hat{\varepsilon}_2 C_1}{2x_{1,b}}\left[2\lambda_0\xi\cos h(\lambda_0\xi) - \sin h(\lambda_0\xi)\right] + k_2 C_2\xi \end{aligned} \tag{A7}$$

where the two constants C_3 and C_4 are not shown here for long expression.

Appendix B: Detailed derivations for SPM

From Eqs. 33 and 34,

$$\begin{aligned} J(\tilde{z}) &= \tilde{x}^{\gamma_1}\left(\frac{1}{x_{1,b}} - \tilde{x}\right)^{\gamma_2}\left[\tilde{x}\exp(\alpha\tilde{\eta}) - \frac{1-x_{1,b}\tilde{x}}{1-x_{1,b}}\exp(-\beta\tilde{\eta})\right] \\ &\approx (1-b\tilde{z})^{\gamma_1}\left(\tfrac{1}{x_{1,b}} - 1 + b\tilde{z}\right)^{\gamma_2} \\ &\times \left\{\left[(1-b\tilde{z})\exp(\alpha Y_0) - \frac{1-x_{1,b}(1-b\tilde{z})}{1-x_{1,b}}\exp(-\beta Y_0)\right]\right. \\ &\left. + \varepsilon\left[(1-b\tilde{z})\alpha\exp(\alpha Y_0) + \frac{1-x_{1,b}(1-b\tilde{z})}{1-x_{1,b}}\beta\exp(-\beta Y_0)\right]Y_1\right\} \end{aligned} \tag{B1}$$

The equations of the overpotential in the scale of $\tilde{z}$ is

$$\varepsilon^2\frac{d^2Y_0}{d\tilde{z}^2} + \varepsilon^3\frac{d^2Y_1}{d\tilde{z}^2} = \varepsilon_1 x_{1,b}^{\gamma_1+\gamma_2} J(\tilde{z}) \tag{B2}$$

Note that the constant $\varepsilon_1 = O(1)$ because of the large thickness of the anode.

The equations and boundary conditions of the overpotential in the coordinate of ζ_1 is

$$\frac{d^2\theta_0}{d\zeta_1^2} + \varepsilon\frac{d^2\theta_1}{d\zeta_1^2} = \varepsilon_1 x_{1,b}^{\gamma_1+\gamma_2} J(\zeta_1), \quad \frac{d\theta_0}{d\zeta_1} + \varepsilon\frac{d\theta_1}{d\zeta_1} = -\varepsilon\frac{Ifl}{\sigma_{ion}^{eff}} \tag{B3}$$

where

$$\begin{aligned} J(\zeta_1) \approx {} & (1-b)^{\gamma_1}\left(\frac{1}{x_{1,b}} - 1 + b\right)^{\gamma_2} \\ & \times \left\{\left[(1-b)\exp(\alpha\theta_0) - \frac{1-x_{1,b}(1-b)}{1-x_{1,b}}\exp(-\beta\theta_0)\right]\right. \\ & \left. + \varepsilon\left[(1-b)\alpha\exp(\alpha\theta_0) + \frac{1-x_{1,b}(1-b)}{1-x_{1,b}}\beta\exp(-\beta\theta_0)\right]\theta_1\right\} \end{aligned} \tag{B4}$$

So, the systems of the zero-order and first-order overpotential are

$$\begin{cases} \dfrac{d^2\theta_0}{d\zeta_1^2} = \varepsilon_1 x_{1,b}^{\gamma_1+\gamma_2}(1-b)^{\gamma_1}\left(\dfrac{1}{x_{1,b}} - 1 + b\right)^{\gamma_2} \\ \quad \times \left[(1-b)\exp(\alpha\theta_0) - \dfrac{1-x_{1,b}(1-b)}{1-x_{1,b}}\exp(-\beta\theta_0)\right] \\ \left.\dfrac{d\theta_0}{d\zeta_1}\right|_{\zeta_1=0} = 0 \end{cases} \tag{B5}$$

$$\frac{d^2\theta_1(\zeta_1)}{d\zeta_1^2} = \lambda_1^2\theta_1 + \frac{\lambda_1^2 b}{(\alpha+\beta)(1-b)\left[1-x_{1,b}(1-b)\right]}\zeta_1, \qquad \left.\frac{d\theta_1(\zeta_1)}{d\zeta_1}\right|_{\zeta_1=0} = -\frac{Ifl}{\sigma_{ion}^{eff}} \tag{B6}$$

where

$$\lambda_1 = \sqrt{\varepsilon_1 x_{1,b}^{\gamma_1+\gamma_2}(1-b)^{\gamma_1+1}\left(\frac{1}{x_{1,b}} - 1 + b\right)^{\gamma_2}(\alpha+\beta)\exp(\alpha\varphi_0)} \tag{B7}$$

The equations and boundary conditions of the overpotential in the coordinate of ζ_2 are

$$\frac{d^2\vartheta_0}{d\zeta_2{}^2} + \varepsilon\frac{d^2\vartheta_1}{d\zeta_2{}^2} = \varepsilon_1 x_{1,b}^{\gamma_1+\gamma_2} J(\zeta_2), \quad \frac{d\vartheta_0}{d\xi_2} + \varepsilon\frac{d\vartheta_1}{d\xi_2} = -\varepsilon\frac{Ifl}{\sigma_{el}^{eff}} \tag{B8}$$

where

$$\begin{aligned} J(\zeta_2) \approx {} & \left(\frac{1}{x_{1,b}} - 1\right)^{\gamma_2}\left\{\left[\exp(\alpha\vartheta_0) - \exp(-\beta\vartheta_0)\right] + \varepsilon\left[\alpha\exp(\alpha\vartheta_0)\right.\right. \\ & \left.\left. + \beta\exp(-\beta\vartheta_0)\right]\vartheta_1\right\} \end{aligned} \tag{B9}$$

So,

$$\frac{d^2\vartheta_0(\zeta_2)}{d\zeta_2{}^2} = \varepsilon_1 x_{1,\mathrm{b}}^{\gamma_1+\gamma_2}\left(\frac{1}{x_{1,\mathrm{b}}}-1\right)^{\gamma_2}[\exp(\alpha\vartheta_0)-\exp(-\beta\vartheta_0)], \quad \left.\frac{d\vartheta_0(\zeta_2)}{d\zeta_2}\right|_{\zeta_2=0} = 0 \tag{B10}$$

$$\frac{d^2\vartheta_1(\zeta_2)}{d\zeta_2{}^2} = \lambda_2^2\vartheta_1 - \frac{\lambda_2^2 b}{(\alpha+\beta)(1-x_{1,\mathrm{b}})}, \quad \left.\frac{d\vartheta_1(\zeta_2)}{d\zeta_2}\right|_{\zeta_2=0} = -\frac{If}{\sigma_{\mathrm{el}}^{\mathrm{eff}}} \tag{B11}$$

where

$$\lambda_2 = \sqrt{\varepsilon_1 x_{1,\mathrm{b}}^{\gamma_1+\gamma_2}\left(\frac{1}{x_{1,\mathrm{b}}}-1\right)^{\gamma_2}(\alpha+\beta)} \tag{B12}$$

Manuscript received Mar. 11, 2007, and revision received July 14, 2007.